Flight table orientation error transparency for hardware-in-the-loop facilities

Nikos Andrianos[a], Christian Diez[b], Louis A. DeMore[a],

[a] Acutronic USA Inc, 139 Delta Drive, Pittsburgh Pennsylvania 15238
[b] Daimler Chrysler Aerospace, LFK GmbH, P.O. Box 801149, 81663 Munich, Germany

ABSTRACT

The addition of flight tables to the HWIL simulation brings with it an "orientation" error that is a function of the table's mechanical misalignments and kinematics. Orientation error is a measure of the overall static inaccuracy of a multi-axis flight table. Combining the orientation error of the three-axis missile flight table with the orientation error of the two-axis target motion table produces a compound orientation error "between" the two independent motion tables. During a typical HWIL missile-to-target engagement scenario, the orientation error will corrupt the computation of guidance & control geometric elements (e.g. the target LOS, the missile airframe orientation angle and the seeker bore-sight angle). We may, with appropriate calibration techniques, make the simulation "transparent" to the motion system orientation error. We also can, with an effective orientation error model, "flow down" requirements to the flight table to reduce the composite orientation error itself. This paper presents the construction of the overall orientation error model based on the measurable table errors of axis wobble, axes non-orthogonality and axis encoding. With this model, the HWIL simulation engineer may, in the future, be able to calibrate and/or set requirements for the missile and target five-axis motion simulator to reduce the effect of the static orientation error on the simulation.

Keywords : flight tables, orientation error, pointing error, wobble, non-orthogonality, axes intersection, encoding error

1. INTRODUCTION

The flight table is just one of several physical effects simulators in the HWIL laboratory. These physical effects simulators include a target scene generator and the real-time simulation computers for the target generation and the 6-DOF missile-target engagement dynamics. Figure 1-1 (shown with permission from the EADS Corporation, LFK GmbH, Munich Germany) is a photograph of the Acutronic Model HD7756 five-axis flight table in the Daimler Chrysler Aerospace laboratory.

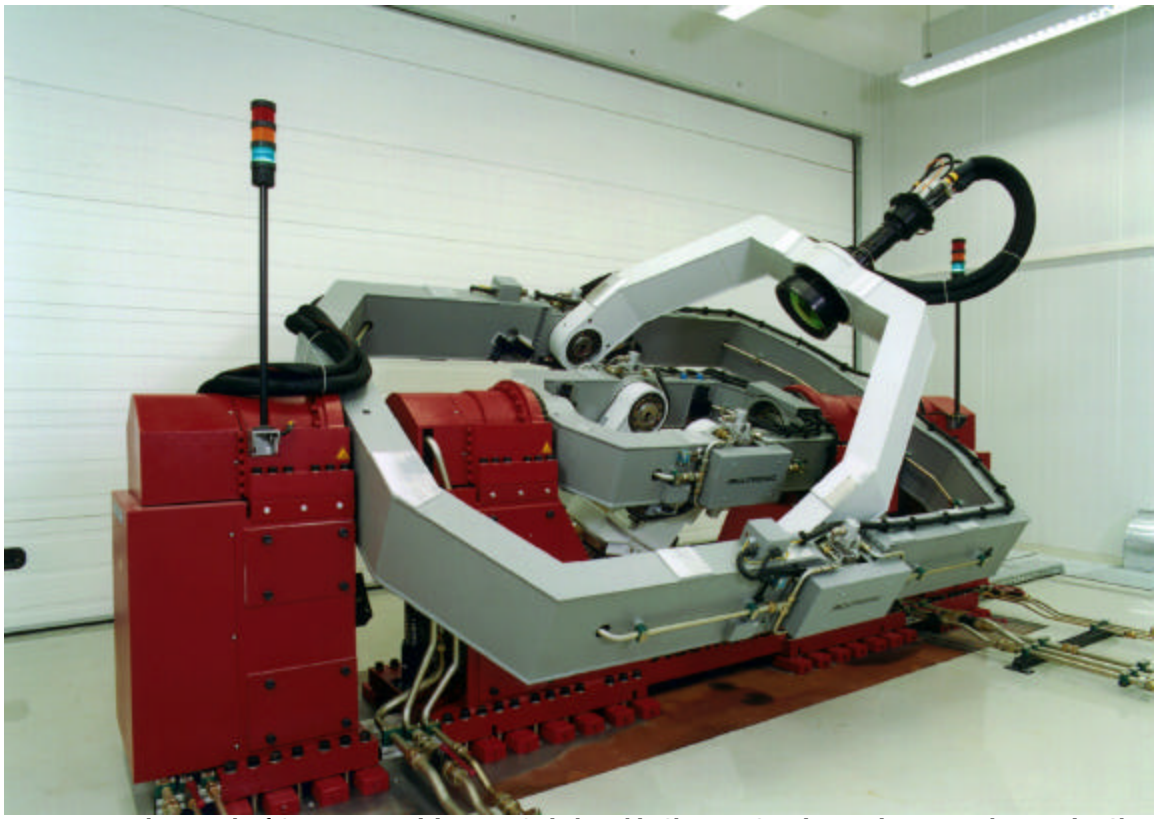

Figure 1-1 Photograph of Acutronic Model HD7756 Flight Table Showing Simulation Elements at the Daimler Chrysler Aerospace LFK HWIL Laboratory

The figure shows the two-axis target motion simulator "wrapped around" the three-axis missile flight table. When this photograph was taken, the Daimler Chrysler simulation engineers had not yet installed the missile seeker into the three-axis flight table. However, the inner gimbal of the target motion simulator contains the collimating optics for the target scene simulator. The alignment and encoding errors of the three-axis and two axis tables will affect the fidelity of the HWIL simulation facility.

We can reproduce a simple illustration of the effect that the flight table orientation error has on the overall HWIL simulation. In "Improvements in Flight Table Dynamic Transparency"[1], we presented a two-dimensional air-to-ground engagement geometry that included the missile airframe orientation dynamics. In Figure 1-2 we consider a two-dimensional ground-to-air engagement geometry with the missile and target simply as points with no body orientation.

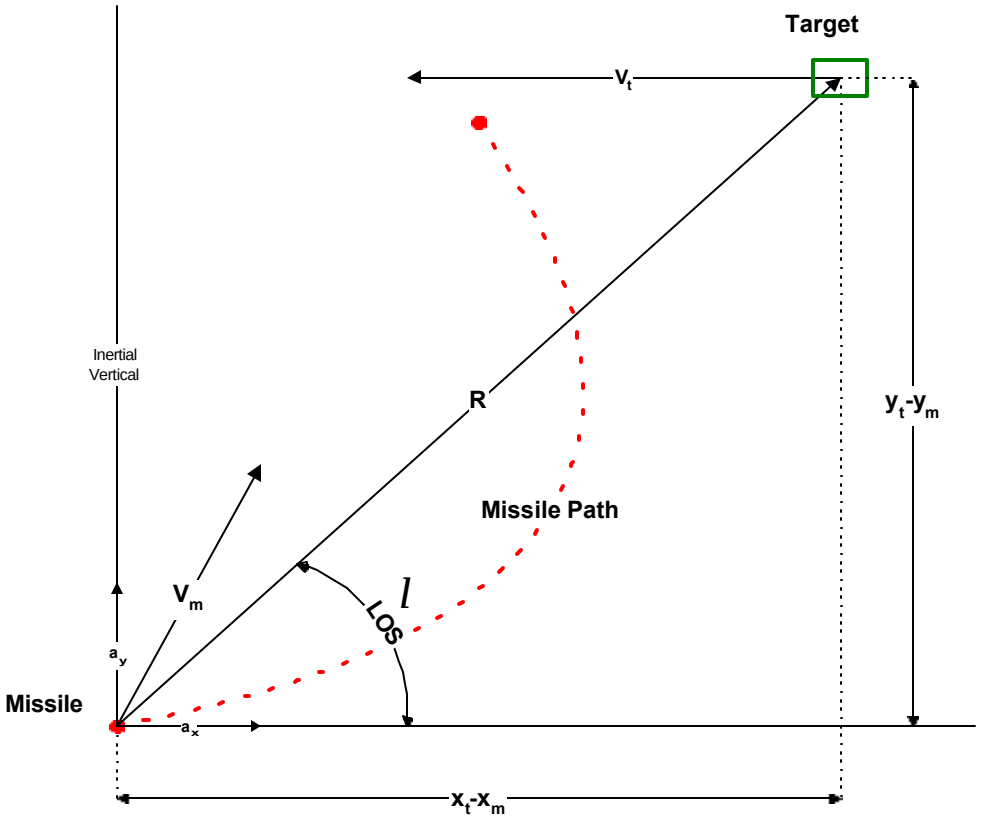

Figure 1-2 Two-Dimensional Missile-to-Target Engagement Scenario Showing the Overall Geometry During the Engagement

From the figure the overall engagement geometry contains the following variables:

1. $l \cong$ *Line-of-Site (LOS) angle, from missile to target*
2. $X_M \cong \begin{bmatrix} x_m \\ y_m \end{bmatrix} \cong$ *missile position vector*
3. $X_T \cong \begin{bmatrix} x_t \\ y_t \end{bmatrix} \cong$ *target position vector*
4. $R \cong$ *range vector from missile to target*
5. $V_M \cong$ *missile velocity vector*
6. $V_T \cong$ *target velocity vector*
7. $a_x, a_y \cong$ *unity basis vectors in the* x *anf* y *directions*

The LOS angle, l, is the angle between the inertial horizontal plane and the range vector, R. Both l and R vary as the engagement plays out. The relationship between l and R, for small l, is simply:

$$\sin(l) = \frac{y_t - y_m}{|R|} \approx l$$

and (1)

$$|R| = \sqrt{(x_t - x_m)^2 + (y_t - y_m)^2}$$

Figure 1-3 is a simplified block diagram of the two-dimensional engagement problem showing the overall missile-to-target engagement geometry. The figure contains a missile seeker and autopilot and uses a proportional navigation tracking algorithm.

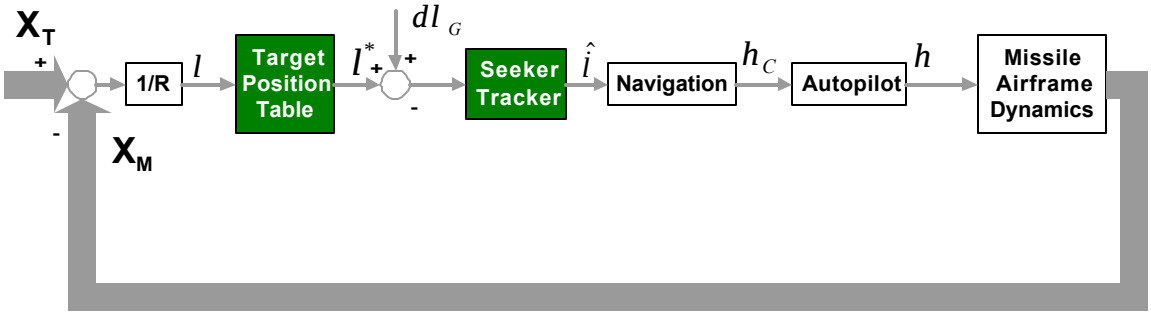

Figure 1-3 Simplified Block Diagram of Two -Dimensional Missile/Target Engagement Showing the Addition of the Gimbal Error to the Estimated LOS

The additional variables in Figure 1-3 are:

1. $l^* \cong$ *simulated LOS Angle*
2. $\hat{\dot{l}} \cong$ *LOS angular rate estimate*
3. $V_c \cong \begin{bmatrix} \dot{x}_m \\ \dot{y}_m \end{bmatrix} \cong$ *missile closing velocity vector*
4. $h_C \cong \begin{bmatrix} \ddot{x}_C \\ \ddot{y}_C \end{bmatrix} \cong$ *normal acceleration command vector to missile*
5. $dl_G \cong$ *LOS error due to target gimbal misalignments*

The missile seeker/tracker generates the LOS angular rate estimate, $\hat{\dot{l}}$. The proportional navigator produces the normal acceleration command, h_C, to the missile autopilot that is proportional to the closing velocity, V_C, and $\hat{\dot{l}}$. The figure also shows the interfaces between the hardware (physical effects) and the software (simulation computer) elements of the simulation laboratory. The variables l^* and dl_G are the target motion table's ideal and error responses to l respectively.

The hardware elements in the figure are shaded and consist of:

- target position table
- missile seeker and tracker

We have created a VisSim computer simulation of the scenario defined by Figure 1-3 in order to investigate the effect of the motion table error, dl_G, on the engagement. We define the missile with rigid body dynamics and the target with point kinematics. We assume that the target remains at a fixed altitude throughout the engagement and that the target and missile are both velocity magnitude limited. The following characteristics further define the engagement scenario:

1. $l_0 \cong$ *initial LOS = 0.3 radians*
2. $|V_M|_0 \cong$ *missile velocity magnitude = Mach 2*
3. $|V_T|_0 \cong$ *target velocity magnitude = Mach 1.5*
4. $|R|_0 \cong$ *initial range magnitude = 3,500 m*

We express the proportional navigation normal control acceleration command as:

$$h_C \cong \begin{bmatrix} \ddot{x}_C \\ \ddot{y}_C \end{bmatrix} \propto \begin{bmatrix} -\hat{\dot{l}}\dot{y}_m \\ \hat{\dot{l}}\dot{x}_m \end{bmatrix}$$

We ran the simulation and computed several different variables including the "miss distance", in the a_y direction given as $(y_t - y_m)$ with gimbal errors $dl_G = \pm 0.05\ degrees$. Figures 1-4a and 1-4b show some of the computer simulation results of the engagement scenario. Figure 1-4a shows the missile "hitting" the target in the a_x, a_y plane. Figure 1-4b shows the "miss distance" in the a_y direction for the gimbal error values.

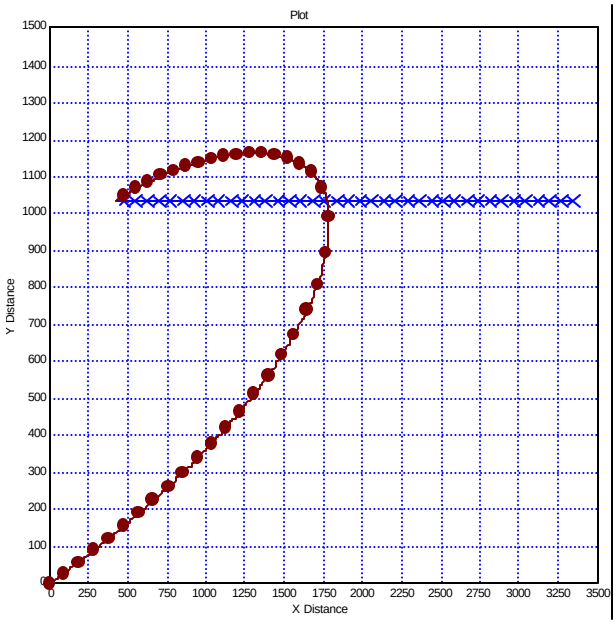

Figure 1-4a Entire Two-Dimensional Missile/Target Engagement Scenario Showing Start to Impact

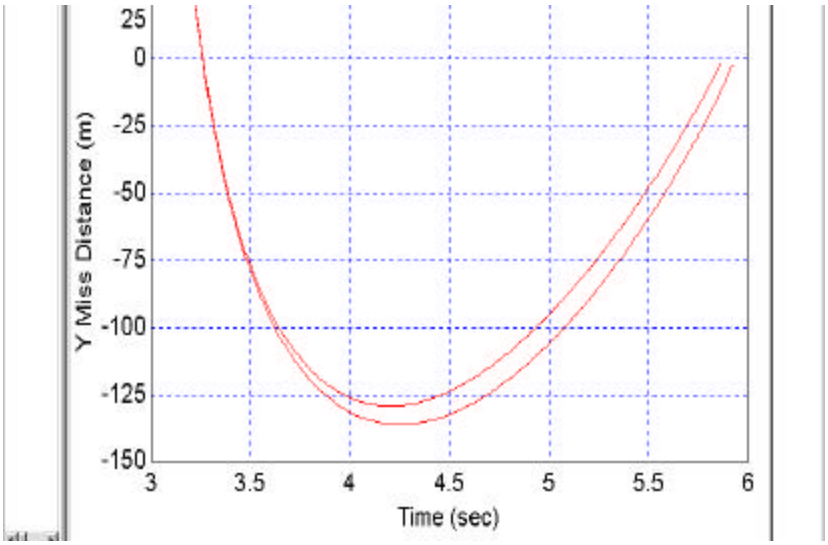

Figure 1-4b End Game "Miss Distance along a_y Direction for the Two-Dimensional Missile/Target Engagement with $dl_G = \pm 0.05\ degrees$ Showing a Maximum Variation of about 15 m

The simulation with the gimbal error produces a difference in the miss distance, as seen from Figure 1-4b, as well as other engagement variables such as "time to hit", and peak LOS rate. The "time-to-hit" and peak LOS rate changed by about 2 % and 3% respectively. In all cases the missile control compensated for the added gimbal induced LOS error and hit the target. By adding the gimbal error to this simple simulation we see the effect of the "non transparency" of target flight table to the simulation.

We increase the realism of the simulation by adding some of the flight hardware to the loop; e.g. the missile seeker and the body rate gyro. Adding the flight hardware also requires the three-axis missile flight table to simulate the missile body orientation and the two-axis target position table to simulate the missile-to-target LOS. The composite orientation error from all five axes of the HWIL flight table could significantly compromise the fidelity of the simulation. This simple two-dimensional example illustrates the effect of only the error from one of the flight table's five axes. When magnified by the additional errors of the entire five-axis flight table, the effect that the target position table and missile flight table will have on the overall fidelity of the simulation emphasizes the need for transparency.

In the following sections of this paper we create separate composite orientation error models for both the three-axis missile flight table and the two-axis target motion table based on the underlying, measurable flight table errors. We can use this composite orientation error model to determine the transparency of any five-axis flight table and ascertain its usefulness as a HWIL element.

2. FLIGHT TABLE MECHANICAL CONFIGURATION

Figure 2-1 shows three-dimensional models of our HWIL flight table.

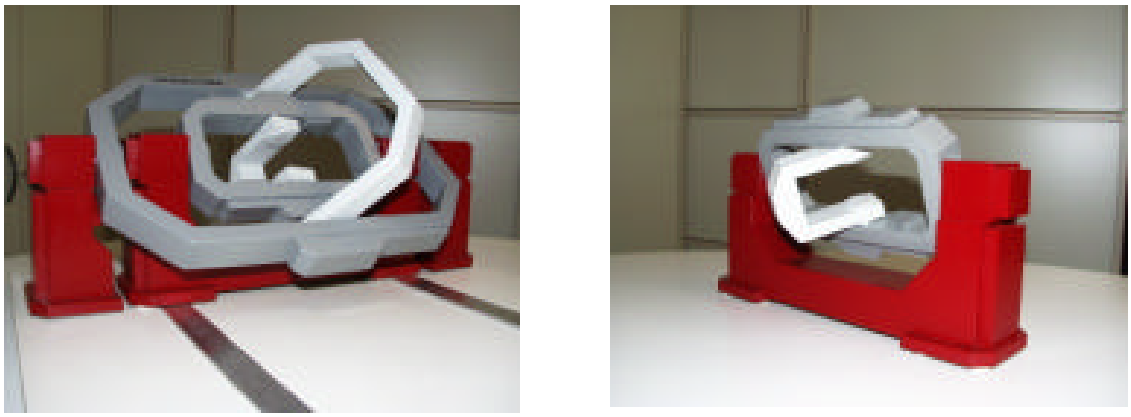

Figure 2-1 Three-Dimensional Models of Acutronic 5-Axis Flight table showing the Five-Axis and the Three-Axis Configurations

The figure shows the configuration of the five-axis flight table on the left and the "stand alone" three-axis missile motion simulator on the right. The inner gimbal structures for the three-axis and two-axis tables, shown as white in the figure, will hold the test missile seeker and the IR target scene simulator on the three and two axis tables respectively. The orientation errors of the missile seeker attached to the inner gimbal of the three-axis table and the target scene simulator attached to the inner gimbal of the two-axis target simulator will corrupt the overall HWIL simulation as illustrated in section 1.0 above. The table manufacturer will routinely measure static axis misalignment and positioning errors in an effort to determine the "accuracy" of the table. We classify these errors as orthogonality error, wobble error and encoding error.

Figures 2-2 and 2-3 show our typical test set-ups to determine the flight table's orthogonality, wobble and encoding error.

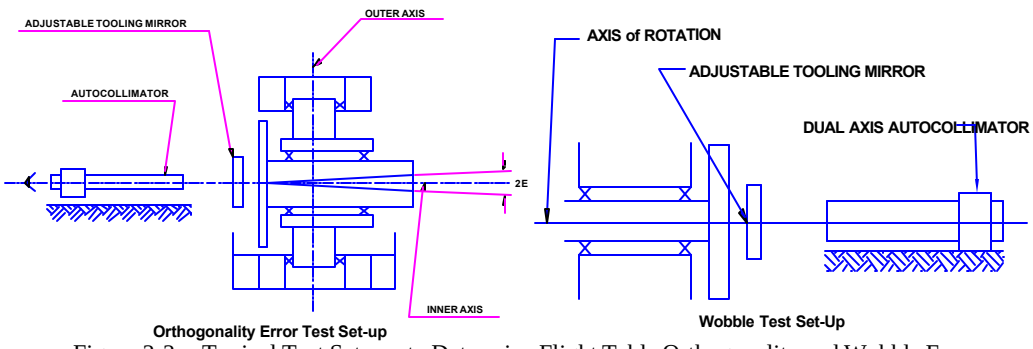

Figure 2-2 Typical Test Set-ups to Determine Flight Table Orthogonality and Wobble Errors

The set-up depicted on the left half of the figure shows how we can measure the perpendicularity error between two intersecting axes; in this case the inner and outer axes. By rotating the inner gimbal about the inner axis and about the outer axis in the proper sequence, and using the autocollimator we can determine the orthogonality error. The set-up shown on the right half of the figure shows how we can measure the axis wobble error. In like manner to the orthogonality error measurement, we observe the output of the dual axis autocollimator while rotating the axis to determine the random wobble error. In both cases the collimating optics must be resolvable to within at least 0.2 arc seconds.

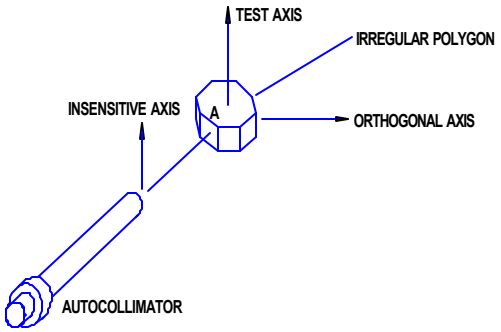

Figure 2-3 Typical Test Set-ups to Determine Flight Table Encoder Errors

We use the position accuracy test set-up shown in Figure 2-3 to measure the encoding error of a multi-pole resolver or Inductosyn®. The set-up uses a calibrated eight sided irregular polygon and the collimator to take the raw data. From eight sets of data we can separate and determine the coarse (once per revolution) and the fine (once per fine cycle) axis angle encoding errors. As in the case of the orthogonality and wobble errors, the collimating optics must be resolvable to at least 0.2 arcseconds.

3. ORIENTATION ERROR MODEL

3.1 Orientation Error for the Three-Axis Table

Orientation error is a measure of the overall rotational, static accuracy of a rate table. By invoking "rotational" as a constraint we exclude the errors associated with the translational motion of relative gimbals or of motion table piers. By invoking "static" as a constraint we exclude the errors associated with the gimbal structural deflections as well as the errors associated with the dynamic tracking of the axes servo systems. "The Design Study for a High-Accuracy Three Axis Test Table"[2], presents a general formulation of "pointing error" for a three axis table. Orientation error is related to pointing error in that they both are functions of the underlying table errors and the rotation through which the gimbals move.

Figure 3-1 is a simplified mechanical sketch of a three-axis table that illustrates a conventional HWIL flight table in a yaw-over-pitch configuration. The perfectly orthogonal basis set, $B = (X_0, Y_0, Z_0)$, represents the original, fixed, coordinate reference frame that is attached to the base of the rate table. The outermost axis is the pitch axis, the innermost axis is the roll axis and the middle axis is the yaw axis. In this configuration the HWIL simulation engineer will attach the missile seeker package to the innermost axis. All gimbals are free to move continuously about their respective axes so that the inner and middle axes will continuously change their orientation with respect to B. In the configuration shown in Figure 3-1, the outer and the inner gimbal axes are locked. At this singularity, the system looses a degree-of-freedom.

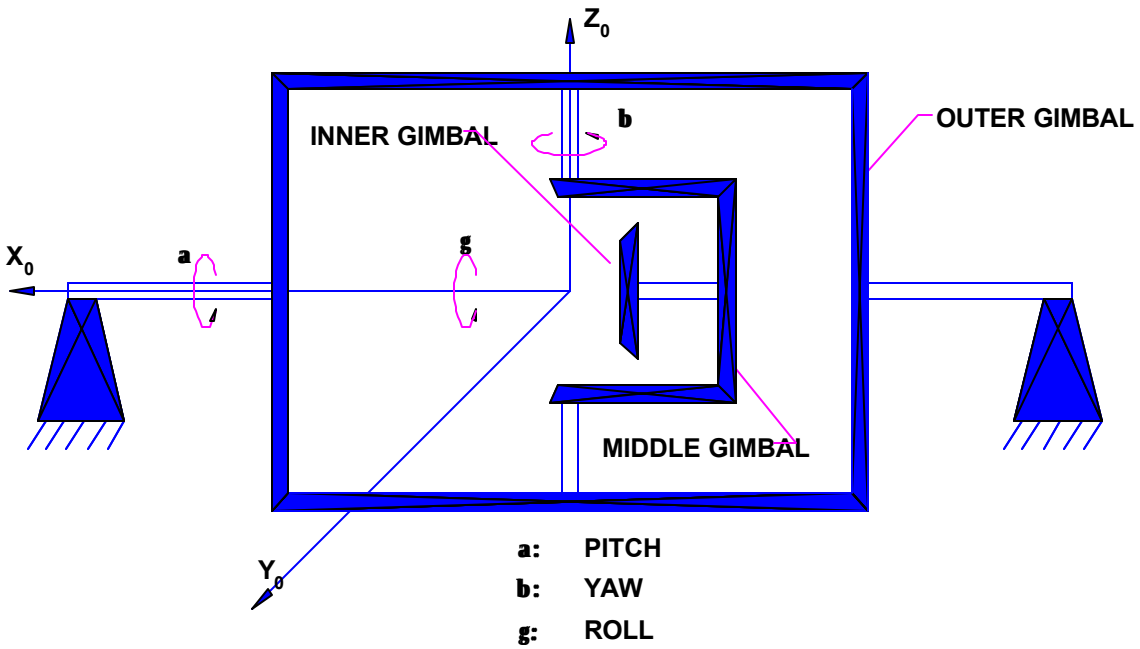

Figure 3-1 Three-Axis Table Configuration Representing a HWIL Missile Flight Table

The geometrical definition of pointing error[2] is the error in the pointing direction of a test unit vector, h_0, that is attached to the innermost gimbal of the simulator. If the gimbals had no errors, a rotation through angles $\Theta = (a, b, g)$ would send the test unit vector h_0 to the vector $h_0(a, b, g)$. Actually, due to the gimbal errors the original vector h_0 ends up in the direction vector $h(a, b, g)$. The pointing error in rotating h_0 is defined as the vector difference

$$dh = h(a, b, g) - h_0(a, b, g) = dR(a, b, g) \cdot h_0 .$$

The rotation error matrix $dR(a, b, g)$ contains the full description of the rotation error as a function of the gimbal angles. However, a good single numerical measure of the "**pointing error**" is the magnitude $|dh|$ of the vector difference, so long as $|dh| << 1$. Now, this error depends not only on the gimbal angles of rotation but also on the initial test unit vector h_0. Because of the configuration of the table axes, a unit test vector in any direction would suffer a different pointing error for the same gimbal angles $\Theta = (a, b, g)$. For this reason we prefer to define an "**average pointing error**" $\bar{d}_p$, which is the average pointing error over all possible initial unit test vectors. In many cases we are not interested merely in the angular error along a pointing direction, but in the overall "**orientation error**" of a solid test package. Again, the full description of the rotation error is contained in the rotation error matrix $dR(a, b, g)$. However, we can extract a single numerical measure of the orientation error from $dR(a, b, g)$ by the use of **Euler's Theorem.** Euler's theorem states that given the ideal, intended final orientation of a test package, and its actual final orientation, there exists a unit direction A and an angle d_O such that a rotation by d_O around A will make the actual package orientation coincide with the ideal intended orientation. We choose this geometrically meaningful quantity d_O as a single numerical measure of orientation error. This measure of orientation error depends not only on gimbal angles but also on the original orientation of the test package. We perform again an average over all possible initial test package orientations to arrive at an overall measure of orientation error. Explicit expressions for $\bar{d}_p$ and d_O will be given below.

The individual simulator errors represented as the error set, $\Xi = (K, W, E)$, affect both the pointing and orientation errors. The error set, sketched in Figure 3-2, is a function of physical misalignments, bearing errors and servo position sensor errors of the flight table. These errors have a definite geometrical relationship to the flight table axes.

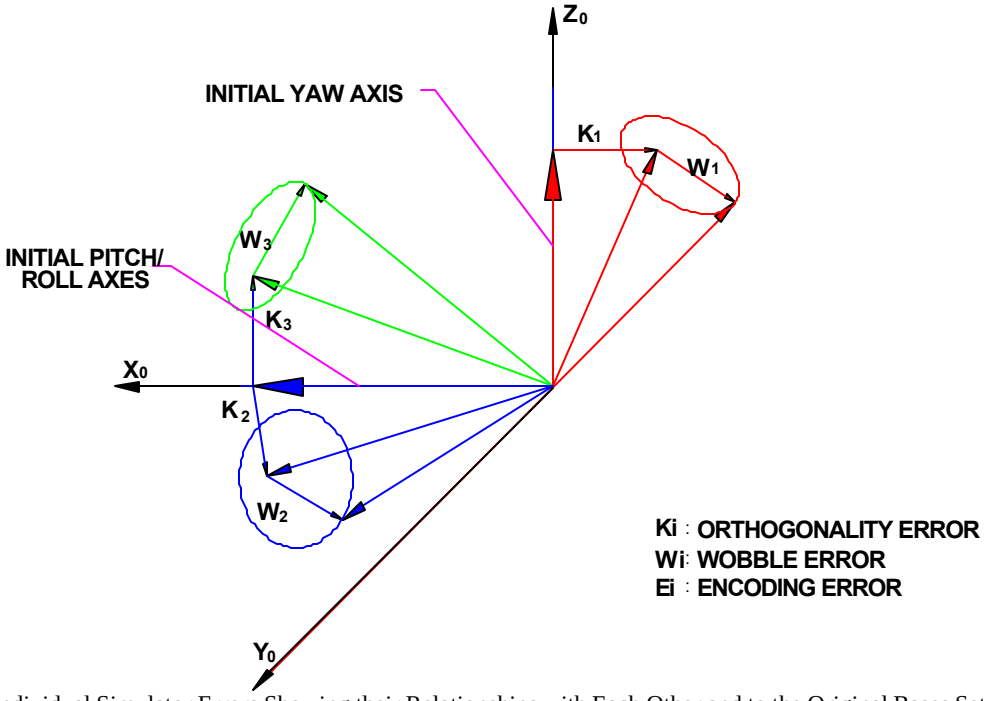

Figure 3-2 Individual Simulator Errors Showing their Relationships with Each Other and to the Original Bases Set for a Three-Axis Rate Table

The error set, Ξ, is composed of the subsets of orthogonality error, K, wobble error, W and encoder error, E. The peak orthogonality errors between the three mutually orthogonal axes make up the orthogonality error subset, i.e.

$$K = (\pm K_1, \pm K_{2,} \pm K_3)$$

The peak axis wobble errors for the three table axes make up the wobble error subset, i.e.

$$W = (\pm W_1, \pm W_{2,} \pm W_3)$$

And finally, the peak axis encoder errors make up the encoder error subset, i.e.

$$E = (\pm E_1, \pm E_{2,} \pm E_3)$$

Figure 3-3 illustrates our definition of orientation error. H_0 is the initial test body with the orientation defined by the body fixed bases vectors: a_x, a_y, a_z. H' represents the intended body orientation after an ideal rotation, and H'' the actual body orientation. The body fixed bases vectors: a_x, a_y, a_z define the intended and actual orientation. The figure shows the relationship of the test body attached to the flight table and what happens as we rotate the gimbals through the angular rotation set, Θ.

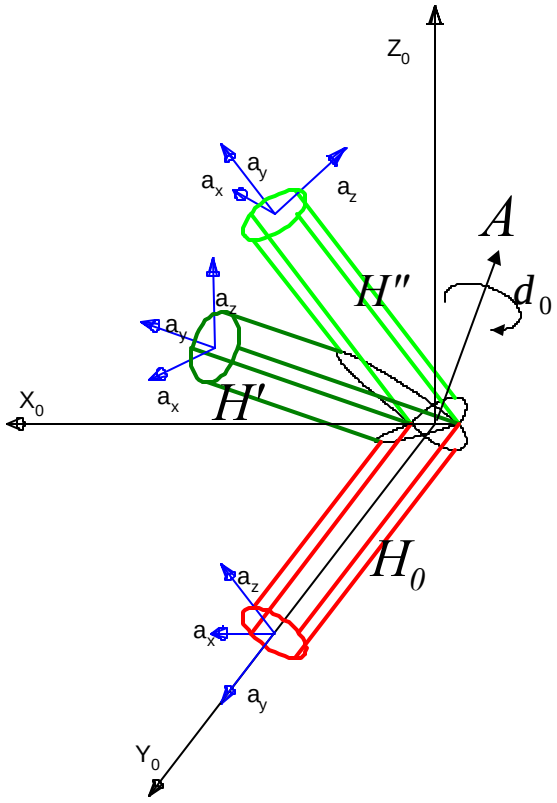

Figure 3-3 Illustration of Orientation Error for a Three-Axis Flight Table

As with any body orientation change, Euler's theorem states that we can always find a vector A and a rotation d_O that will make the body H'' coincide with H'. We define the angle d_O, which moves the test body located at orientation H'' to the orientation H', as the orientation error. The square of the orientation error magnitude is given as:

$$d_O^2 = \frac{1}{2} Tr\{dR^T dR\} \qquad (2)$$

where dR is the error rotation (direction cosine) matrix[2], i.e.

$$dR \equiv R(\Theta) - R(\Theta, \Xi)$$

where $R(\Theta)$ is the appropriate direction cosine matrix.

In the case of pointing, the square of the pointing error averaged over all initial pointing directions is simply

$$\bar{d}_p^{\,2} = \frac{1}{3} Tr\{dR^T dR\}$$

and the maximum value of this average pointing error for the worst case combination of table orientation and signed individual table errors is:

$$\bar{d}_{p\max} = \max_{\Theta,\Xi} \{\bar{d}_p\}$$

We can do the same for orientation error. So the maximum orientation error is

$$d_{O\max} = \max_{\Theta,\Xi} \{d_O\} \qquad (3)$$

Figure 3-4 illustrates the orientation error for a three-axis flight table as a function of gimbal movement. In this case we assume that the flight table has only orthogonality errors of 1 arcsec per axis. We ignore the wobble and encoding errors.

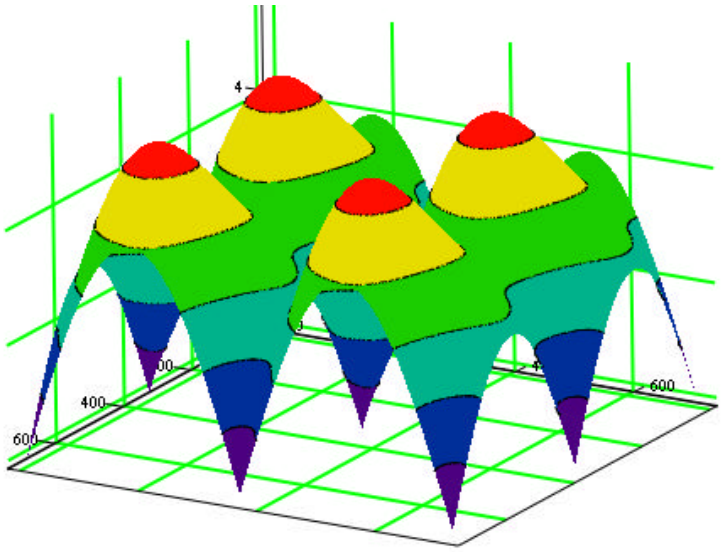

Figure 3-4 Plot of $\sqrt{Tr\{dR^T dR\}}$ versus gimbal motion, $b = 0$ *to* 720, $g = 0$ *to* 720, for Orthogonality Error of 1 arcsec illustrating Orthogonality Dominated Orientation Error for a Three-Axis Flight Table

The figure plots the term $\sqrt{Tr\{dR^T dR\}}$ as a function of (b, g); the error is independent of a . The maximum value from the figure is about 5.4 arcsec, so the maximum orientation error would be:

$$d_{O\max} = \frac{1}{\sqrt{2}}\sqrt{Tr\{dR^T dR\}}\Big|_{\max} = 0.707 \times 5.4 \approx 3.8 \; arcsec$$

We assume the flight table has three orthogonality errors representing misalignments of the three planes: XY, XZ, and ZY. We generally measure two of the three misalignments by measuring the in-plane, non-orthogonality errors between the middle and the outer axes and between the middle and inner axes as described in Section 2 above. We generally ignore the "out-of-plane" errors that would give us the third plane misalignment information. A computational algorithm was developed to solve equation (3). The algorithm searches for the maximum orientation error over all possible table orientations for a given set of flight table errors. In the case where we only measure two orthogonality errors, we create a third from the larger of the two by using the error's two equal normal components. That is:

$$K_i = \frac{K_M}{\sqrt{2}}, \; i = 1,2$$

where K_1 and K_2 are the normal error components of the measured error, K_M . Table 3-1 gives the results of the orientation error estimate from equations (2) and (3) for encoding, wobble and orthogonality zero-to-peak errors equal to 1 arc sec each. We see the orientation error for the individual errors and for the composite.

Table 3-1 Composite Orientation Error Sensitivity for a Three-Axis Table

Zero to Peak Error Source per axis (Arc Sec)			Average Maximum Orientation Error, $d_{O\max}$, for a 3-Axis Rate Table (Arc Sec)
Encoder	Orthogonality	Wobble	
1	0	0	2.2
0	1	0	3.8
0	0	1	2.2
1	1	1	5.8

We use the individual data to measure the sensitivity of the orientation error to the encoder, wobble and orthogonality errors. The orientation error is at least 60% more sensitive to the orthogonality error than it is to either the encoder or wobble errors.

3.2 Orientation Error for the Two-Axis Table

Figure 3-5 is a mechanical sketch of a two-axis table that illustrates a conventional HWIL target motion table in a azimuth-over-elevation configuration. The orthogonal bases set, $B = (X_0, Y_0, Z_0)$, represents the original, fixed, coordinate reference frame that is attached to the base of the rate table and is consistent with the missile seeker, three-axis flight table shown in Figure 3-1. The outer axis of the two-axis table is the elevation axis and the inner axis is the azimuth axis. In this configuration the HWIL simulation engineer attaches the target scene generator package to the inner axis. All gimbals are free to move about their respective axes so that the inner and middle axes will continuously change their orientation with respect to B.

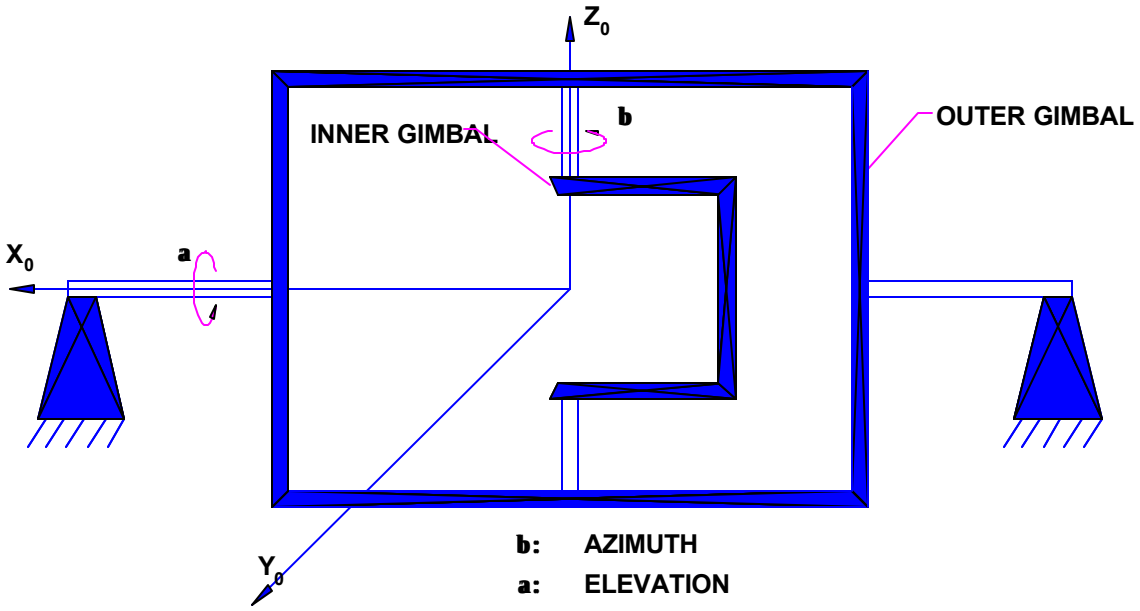

Figure 3-5 Two-Axis Table Configuration Representing the HWIL Target Motion Simulator

The orientation error for the two-axis target motion table simply reduces to the orientation error for the three-axis table without the innermost axis. Equations (2) and (3) are equally valid for the two axis case; but we must recognize that the error matrix, dR, is just a function of the two axis rotation set $\Theta_2 = (a, b)$ and the limited error set $\Xi_2 = (K_2, W_2, E_2)$ with just two errors each for the wobble and encoder and one error for orthogonality. Figure 3-6 is a repeat of Figure 3-4 for the orientation error for a two-axis table with only orthogonality errors. Again we neglect the wobble and encoding errors.

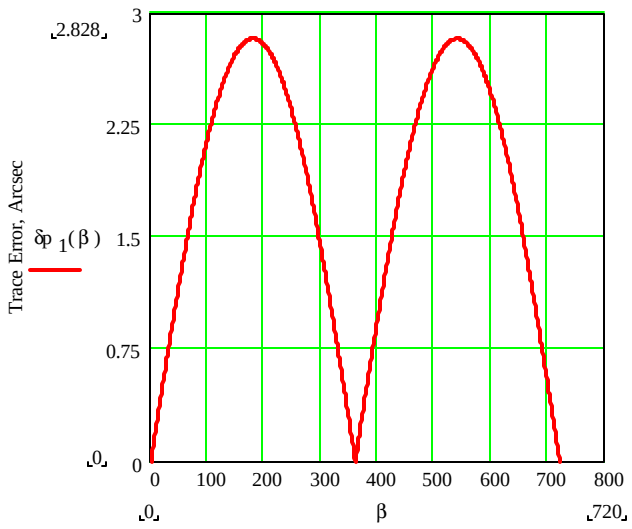

Figure 3-6 Plot of $\sqrt{Tr\{dR^T dR\}}$ versus gimbal motion, $b = 0$ *to* 720, for Orthogonality Error of 1 arcsec illustrating Orthogonality Dominated Orientation Error for a Two-Axis Flight Table

In this reduced case, the orientation error is only a function of the inner axis angle, b, and the single orthogonality error. The peak occurs when the middle axis moves through 180 degrees. As in the previous figure, this figure plots the term $\sqrt{Tr\{dR^T dR\}}$ as a function of b. The maximum value from the figure is about 2.8 arcsec, so the maximum orientation error would be:

$$d_{O\max} = \frac{1}{\sqrt{2}}\sqrt{Tr\{dR^T dR\}}\Big|_{\max} = 0.707 \times 2.8 \approx 2 \; arcsec$$

Table 3-2 gives the results of the orientation error calculation for encoding wobble and orthogonality zero-to-peak errors equal to 1 arc sec each. We see the orientation error for the individual errors and for the composite.

Table 3-2 Composite Orientation Error Sensitivity for the Two-Axis Table

Zero to Peak Error Source per axis (Arc Sec)			Maximum Orientation Error, $d_{O\max}$, for a 2-Axis Rate Table (Arc Sec)
Encoder	Orthogonality	Wobble	
1	0	0	1.4
0	1	0	2.0
0	0	1	1.4
1	1	1	3.1

We see similar results between the three-axis and two-axis cases. The orientation error in Table 3-2, just as the data shows in Table 3-1, is at least 60% more sensitive to the orthogonality error then it is to either the encoder or wobble errors.

3.3 Composite Orientation Error for the Five-Axis Table

In Sections 3.1 and 3.2 above we developed the orientation error for the three-axis table and the two-axis table individually. Since we use the two motion tables to simulate two independent operations in the HWIL laboratory; we can also justifiably treat the orientation errors independently. Specifically, the two-axis table errors will corrupt the simulation of the target-to-missile line-of-sight while the three-axis table errors will corrupt the simulation of the missile body orientation. We can also, as a figure of merit, construct a measure of the composite orientation error for the combined five-axis motion simulator.

Figure 3-7 illustrates the vector sum of the three-axis and the two-axis orientation errors.

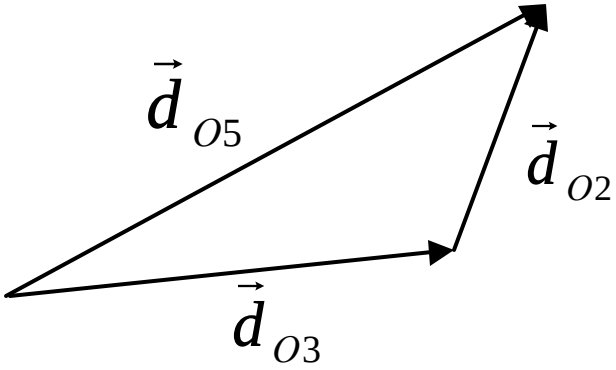

Figure 3-7 Illustration of Composite Orientation Error as the Sum of the Three-Axis and Two-Axis Table Orientation Errors

We treat the orientation errors as vectors because the independent errors for the two and three axis tables may add or subtract depending on their relative orientations. We represent the composite orientation error for the five-axis simulator, $\vec{d}_{O5}$,as a vector sum, i.e.:

$$\vec{d}_{O5} = \vec{d}_{O2} + \vec{d}_{O3}$$

where $\vec{d}_{O2}$ and $\vec{d}_{O3}$ are the two and three axis table orientation error vectors respectively. The magnitude of the composite will be a maximum when the individual table orientation errors point in exactly the same direction. Conversely, the composite will be minimum when the individual table orientation errors point in exactly the opposite direction. As a compromise, we can create a useful measure of the composite by considering the individual table errors orthogonal to each other. In this case the magnitude of the composite is given by;

$$d_{O5}^2 = d_{O2}^2 + d_{O3}^2 \qquad (4)$$

We can compute the composite from equation (4) and using equations (2) and (3) above.

4. SUMMARY

Mechanical misalignments and axis encoding errors have always been defining criteria in determining the acceptable performance level of flight tables used in HWIL laboratories. We have defined a composite orientation error for the flight table that can be used very effectively as a single performance criterion. We described a tool that permits us to estimate the orientation error of a HWIL flight table given the underlying, measurable table errors in axis orthogonality, wobble and encoding. The composite orientation error of a motion table is almost impossible to measure directly so this tool is extremely helpful in determining the transparency of the flight table to the HWIL simulation. We may also be able to use the error model as a point-wise calibration tool to compensate for the table errors during the HWIL simulation. This latter use of the composite orientation error model is much more challenging in that the contributing errors of wobble and orthogonality need to be characterized in a point-wise sense to be properly used in the model.

5. ACKNOWLEDGEMENTS

The authors wish to thank Daimler Chrysler Aerospace, LFK GmbH, P.O. Box 801149, 81663 Munich, Germany for permission to use the photograph of the flight table in the HWIL laboratory shown in Figure 1-1.

6. REFERENCES

1. Louis A. DeMore, Paul Mackin, Michael Swamp, Roger Rusterholtz, “Improvements in Flight Table Dynamic Transparency for Hardware-in-the-Loop Facilities”, Proceeding of SPIE Vol.4027 (2000), presented at Aerosense 2000, 24-26 April 2000
2. Louis A. DeMore, R.A. Peterson, L.B. Conley, H.H. Havlicsek, N.P. Andrianos, D.H. Ditto, J. Profeta III. “ Design Study for a High-Accuracy Three-Axis Test Table” AIAA Journal of Guidance, Control and Dynamics, VOL. 10, NO. 1, Jan.-Feb. 1987